HHS Public Access

Author manuscript

Dev Biol. Author manuscript; available in PMC 2022 June 02.

Published in final edited form as:

Dev Biol. 2021 August ; 476: 18–32. doi:10.1016/j.ydbio.2021.03.008.

Spatiotemporal mapping of sensory and motor innervation of the embryonic and postnatal mouse urinary bladder

Casey JA Smith-Anttila[1], **Victoria Morrison**[1], **Janet R Keast**[1]

[1]Department of Anatomy and Neuroscience, University of Melbourne, Melbourne, Victoria, Australia

Abstract

The primary function of the urinary bladder is to store urine (continence) until a suitable time for voiding (micturition). These distinct processes are determined by the coordinated activation of sensory and motor components of the nervous system, which matures to enable voluntary control at the time of weaning. Our aim was to define the development and maturation of the nerve-organ interface of the mouse urinary bladder by mapping the organ and tissue distribution of major classes of autonomic (motor) and sensory axons. Innervation of the bladder was evident from E13 and progressed dorsoventrally. Increasing defasciculation of axon bundles to single axons within the muscle occurred through the prenatal period, and in several classes of axons underwent further maturation until P7. Urothelial innervation occurred more slowly than muscle innervation and showed a clear regional difference, from E18 the bladder neck having the highest density of urothelial nerves. These features of innervation were similar in males and females but varied in timing and tissue density between different axon classes. We also analysed the pelvic ganglion, the major source of motor axons that innervate the lower urinary tract and other pelvic organs. Cholinergic, nitrergic (subset of cholinergic) and noradrenergic neuronal cell bodies were present prior to visualization of these axon classes within the bladder. Examination of cholinergic structures within the pelvic ganglion indicated that connections from spinal preganglionic neurons to pelvic ganglion neurons were already present by E12, a time at which these autonomic ganglion neurons had not yet innervated the bladder. These putative preganglionic inputs increased in density prior to birth as axon terminal fields continued to expand within the bladder tissues. Our studies also revealed in numerous pelvic ganglion neurons an unexpected transient expression of calcitonin gene-related peptide, a peptide commonly used to visualise the peptidergic class of visceral sensory axons. Together, our outcomes enhance our understanding of neural regulatory elements in the lower urinary tract during development and provide a foundation for studies of plasticity and regenerative capacity in the adult system.

Keywords

urinary tract; parasympathetic; sympathetic; visceral afferent; major pelvic ganglion; inferior hypogastric plexus

Corresponding author: Professor Janet R Keast, Department of Anatomy and Neuroscience, University of Melbourne, Vic 3010, Australia, janet.keast@unimelb.edu.au.
Current affiliation: Dr Smith-Anttila, Walter and Eliza Hall Institute, Royal Parade, Parkville, Vic 3000 Australia.

1. Introduction

Diverse populations of sensory and motor (autonomic) nerves in the urinary bladder are essential for normal continence, voiding and signalling tissue damage (nociception) (Andersson, 2016; Beckel and Holstege, 2011b; de Groat and Yoshimura, 2015; Gonzalez et al., 2014). Dysregulated growth of these axons is associated with clinical conditions such as bladder hyperactivity and pain, whereas loss of innervation due to direct damage (e.g., during pelvic surgery) or disease (e.g., diabetes) severely impairs control of voiding and continence. In order to devise strategies for normalising function or repairing these circuits, it is valuable to understand the factors that drive initial connectivity of the bladder innervation during development. This includes understanding the intrinsic ability of each neuron type to grow axons into each tissue and the synchronisation (or otherwise) of this growth across nerve classes. Likewise, in the context of organ regeneration technology, new strategies to enhance not only nerve growth but appropriately targeting of this growth will be informed by defining these normal processes.

In contrast to the large body of work on the developing enteric nervous system (nerves of the digestive tract) and the mechanisms underlying this connectivity (Uesaka et al., 2016), much less information is available on the developing nervous system of the lower urinary tract. Both sensory and autonomic nerves are present prior to birth (Wiese et al., 2017) and postnatally a spinal, stretch-driven reflex is replaced by a supraspinal reflex that allows integration with other behaviours and determines voluntary voiding (de Groat and Yoshimura, 2015). Bladder voiding and sensation prior to birth have been poorly defined. Therefore, the *first aim* of this study was to define, using pan-neural markers, the timeline and pattern of bladder innervation from the period of initial axon entry to the mature state. Much of our current detailed understanding of the structural features of bladder innervation in adults is derived from studies on rats or guinea pigs, however we have conducted this study in male and female mice, to provide a fundamental dataset for basing future genetic or pharmacological perturbation studies.

Each type of bladder tissue is innervated by both sensory and motor (autonomic) nerves, the distribution and relative density of which vary across tissues and, in some cases within different regions of the bladder. For example, the sensory nerves that distribute near the basal aspect of the urothelium are much more prevalent in the bladder base and neck than in the bladder body (Forrest et al., 2014; Gabella and Davis, 1998; Gillespie et al., 2006). Moreover, sympathetic and parasympathetic classes of motor axons have distinct distributions, aligned with their function. Parasympathetic nerves that mediate contraction during voiding are prevalent in the detrusor of the bladder body but sympathetic nerves that contribute to continence are sparsely distributed in the muscle, yet more prevalent in the bladder neck (Beckel and Holstege, 2011a). Therefore, our *second aim* was to determine whether sensory, sympathetic and parasympathetic innervation occurred simultaneously or showed distinct temporal features. We addressed this by utilising well-established markers of key populations of sensory and autonomic axons to separately track their development, and a reporter line to visualise the marker of a major group of visceral nociceptor axons, TRPV1 (Franken et al., 2014; Gebhart and Bielefeldt, 2016; Grundy et al., 2019). We

extended this component of the study through the postnatal period and compared with adult innervation patterns, in both male and female mice.

The majority of autonomic axons in the bladder originate from neuronal cell bodies located in the pelvic ganglion (PG), also known in rodents as the major pelvic ganglion or, in humans, the inferior hypogastric plexus (Ernsberger et al., 2020; Keast, 1999). This mixed sympathetic-parasympathetic ganglion comprises a mixture of noradrenergic and cholinergic neurons, each with spinal inputs from distinct regions. Separate populations of PG neurons innervate the lower urinary and intestinal tracts, and reproductive organs. The fundamental features of the developing mouse PG have been described previously (Anderson et al., 2006; Georgas et al., 2015; Wiese et al., 2017; Wiese et al., 2012). To facilitate interpretation of axon patterning in the bladder during development and maturation, our *third aim* was to define the expression of primary neural markers in the PG of male and female mice. This set of observations also provided the opportunity to identify the emergence of structures that potentially represent connectivity from spinal preganglionic pathways over this period.

2.0 Materials and Methods

2.1 Animals

All procedures complied with the Australian Code for the Care and Use of Animals for Scientific Purposes (National Health and Medical Research Council of Australia) and were approved by the Animal Ethics Committee of the University of Melbourne. The animals were housed at 21–22°C under a 12h light/dark cycle and provided ad libitum access to food and filtered water.

Adult C57Bl/6 mice were purchased from the Animal Resources Centre (ARC; Western Australia). Heterozygous *TrpV1*$^{\text{PLAP-nLacZ}}$ mice originally generated and validated by Cavanaugh et al. (Cavanaugh et al., 2011) were purchased from JAX® Mice (B6.129-*Trpv1*^{tm2Bbm}/J, Stock #017623), raised on a C57Bl/6 background and maintained as a homozygous line.

2.2 Tissue collection and processing

A minimum of 3 animals was analysed per marker at each age and sex. Tissues were collected from C57Bl/6 mice at E12, E13, E14, E16, E18, P2, P7 and adult (6–10 weeks); *TrpV1*$^{\text{PLAP-nLacZ}}$ mice at E16, E18, P2 and adult (6–10 weeks). Tissues from embryonic and early postnatal mice were fixed by immersion in 4% paraformaldehyde in phosphate buffer (0.1M, pH 7.4) at 4°C for 18–24h, except for tissues from *TrpV1*$^{\text{PLAP-nLacZ}}$ to be used for placental alkaline phosphatase [PLAP]) staining that were fixed for only 4h. Tissues from P28 and adult mice were fixed by transcardial perfusion with 4% buffered paraformaldehyde, following anaesthesia with ketamine and xylazine (150 mg/kg and 15 mg/kg, respectively); following perfusion, tissues were post-fixed for a further 18–24h in the same fixative at 4°C.

All tissues to be studied in sections were cryoprotected for 18–24h in phosphate buffered saline (PBS; 0.1M, pH 7.4) containing 30% sucrose before being embedded in OCT (Tissue-Tek, Sakura, Torrance, CA, USA) and sectioned at 14 μm on a cryostat. Bladder tissue

was also removed from adult *TrpV1*$^{PLAP\text{-}nLacZ}$ mice for visualisation of nerves in whole thickness preparations; here, the bladder was opened along the ventral midline and pinned out, slightly stretched, in Petri dishes lined with silicon polymer; this was followed by fixation for 18–24h at 4°C. Fixed tissues were washed with PBS and stored at 4°C until use.

2.3 Placental alkaline phosphatase (PLAP) Staining

For PLAP staining, sections were washed in PBS to remove the OCT. For adult tissue only, sections were then briefly dipped for 5s in 20% acetic acid at 4°C, before being washed with PBS to fully inactivate endogenous alkaline phosphatases. For all tissue ages, endogenous alkaline phosphatases were inactivated by heating the sections in PBS at 72°C for 90 min. Sections were rinsed in alkaline phosphatase buffer (100 mM Tris-HCl pH 9.5, 100 mM NaCl, 50 mM $MgCl_2$) at room temperature for 10 min prior to colour development with BCIP/NBT (Roche, Hawthorn Vic Australia) in alkaline phosphatase buffer, overnight at room temperature according to the manufacturer's instructions. Sections were washed thoroughly then mounted in buffered glycerol and visualised on the MetaSystems V-Slide scanner at 20X magnification and extracted using VSViewer version v2.1.103 software. Extracted images underwent minor adjustments to levels to using Adobe Photoshop software to ensure close matching to labelling as viewed directly down the microscope. A minimum of four non-consecutive sections per sample were examined.

2.4 Immunohistochemistry

For immunohistochemistry, sections were washed in PBS and incubated for 1h at room temperature with PBS containing 10% non-immune horse serum (Sigma-Aldrich now Merck, North Ryde NSW Australia) and 0.1% Triton X-100. Sections were washed then incubated for 18–24h at room temperature with the primary antibodies listed in Table 1, diluted in hypertonic PBS (PBS containing 17g NaCl per litre). Slides were washed in PBS prior to being incubated with Alexa Fluor® (AF) secondary antibodies: donkey anti-rabbit AF488 (Jackson; Cat# 711-545-152), donkey anti-goat AF594 (Jackson; Cat# 705-585-003) or donkey anti-chicken AF647 (Jackson; Cat# 703-605-155) diluted 1:1000 in hypertonic PBS, for 2.5h at room temperature. Slides were then washed in PBS, incubated with 4,6-diamidino-2-phenylindole (DAPI) (Sigma-Aldrich), washed in PBS, and mounted in buffered glycerol. Images were captured with a Zeiss AxioImager M2 microscope and AxioCam MRm camera using Zen software (Carl Zeiss). Where required, minor adjustments were made in images using Adobe Photoshop, to ensure close matching to labelling as viewed directly down the microscope. A minimum of four non-consecutive sections per sample were examined for each antibody.

2.5 Data communication

The primary data underpinning this study are publicly available in the NIH-funded database, The Genitourinary Development Molecular Anatomy Project, GUDMAP (www.gudmap.org). Many other additional images are available at this site, including documentation of negative data (e.g., lack of innervation by specific nerve populations early in development) and data from both sexes. Detailed protocols for immunohistochemistry and PLAP labelling are also available here.

3.0 Results

3.1 Mapping the total population of bladder axons during embryonic development

We first used the pan-neural marker, PGP (protein gene-product 9.5; *Uchl1*) to generate a spatiotemporal map of the entire population of neuronal structures within the developing bladder, from E13-E18. PGP immunolabelling was also present in the urothelium during this period. Representative data are shown in Figure 1. We did not identify any difference between male and females in the patterning or timing of bladder innervation prior to birth.

As reviewed previously (Georgas et al., 2015), smooth muscle cells detectable by expression of *Acta2* are present in the primitive bladder at E13 but do not form a distinctive compact layer (detrusor) until E14. E13 was the earliest time that axons could be identified within the bladder (Fig. 1a). Axons were restricted to the most dorsal region and were primarily located in multi-axonal tracts near the serosal surface. Single axons were rarely seen. At E14, axons were distributed throughout most of the dorsoventral axis of the muscle but showed a graded transition of decreased axon density from the dorsal to the ventral midline (Fig. 1b, e). In the dorsal bladder, the majority of neuronal structures were located in the muscle and comprised of multi-axon tracts of diverse thickness and rare single axons. At this time, axons began to populate the ventral muscle, in a sparse network of thin tracts and single axons. The axon density in bladder muscle was lower in the dome than more caudal bladder regions. Axons in the lamina propria were rare and only identified in the dorsal bladder. No axons reached the urothelium. By E16, each layer of the bladder showed more extensive innervation than at E14 (Fig. 1c, f). In both the muscle and the lamina propria, axons were present around the complete circumference of the bladder, including a sparse supply associated with the vasculature. Axons in the lamina propria rarely projected to the region near the urothelium. At E18 the innervation of muscle and vasculature appeared similar to E16 (Fig. 1d, g). At this stage, axons were still rarely identified near the urothelium but could be occasionally seen near the urothelium of the bladder neck.

As described in more detail below, we then mapped several major functional classes of axons, inferred from their immunoreactivity to various peptides and proteins previously characterised in adult visceral nerves. For each class, the changes during development followed a broadly similar patterning of the total innervation shown by the pan-neural marker, i.e., an earlier innervation of the dorsal bladder, progressively populating the ventral regions, and innervation of the detrusor muscle prior to the lamina propria and lastly, where innervated, the urothelium. However, differences in tissue innervation and timing were revealed by visualisation of these distinct axon classes. We therefore extended the next step of our study to postnatal maturation (P2, P7) and, as a comparator, the adult bladder. In summary, each class of axons showed an increasing density in specific tissues across the period from E18 to P7, but no further change in patterning or density was evident from P7 to adulthood. We did not identify any consistent sex difference in these innervation profiles.

3.2 Development and maturation of autonomic innervation of the bladder

The predominant class of autonomic axons in the adult bladder is cholinergic, providing excitatory innervation to the detrusor and inhibitory innervation to the bladder neck and

urethra smooth muscle (Beckel and Holstege, 2011b; de Groat and Yoshimura, 2015) there is also a sparser supply to the urothelium, more pronounced at the bladder neck (Dickson et al., 2006). We identified these axons by immunoreactivity for VAChT (vesicular acetylcholine transporter; *Slc18a3*) (Fig. 2). This labelled varicose structures typical of visceral motor innervation that is characterised by multiple transmitter storage and release sites along their terminal axons (Gabella, 1995). Cholinergic axons were absent from the bladder at E13, even though VAChT expression was evident in the pelvic ganglion by this time (see Section 3.4). By E16 there was a moderate innervation of the muscle, more pronounced in its dorsal aspect; at this time, axons in the lamina propria were still rare (Fig. 2a). Muscle innervation increased by E18, but the lamina propria remained sparsely innervated (Fig. 2b). At P2, muscle innervation was of similar density to E18, but urothelial innervation had increased (Fig. 2c, f). By P7 (Fig. 2d, g) the innervation of both tissues had increased significantly and more closely resembled the adult innervation density (Fig. 2e). At all stages where cholinergic axons were present in the lamina propria, they were more prevalent towards the bladder neck.

In adults, a major subgroup of peripheral cholinergic axons co-express nNOS (neuronal nitric oxide synthase; *Nos1*) and VIP (vasoactive intestinal peptide, *Vip*) (Ernsberger et al., 2020). Representative images of nitrergic axons are shown in Figure 3. Nitrergic axons were not identified in the bladder at E13, even though pelvic ganglion neurons expressed nNOS by this time (See Section 3.4). By E16, nitrergic axons were present in the bladder muscle, more prevalent in the dorsal than the ventral aspect and increasing in density towards the bladder neck; at this stage of development, nitrergic axons were sparse in the lamina propria and none were found near the urothelium (Fig. 3 a, b). Innervation of all bladder tissues continued to increase in density from E18 (Fig. 3c, d). Muscle innervation was higher at P2 than E18 but did not appear to increase further from this time; lamina propria innervation was also higher at P2 than E18 but urothelial innervation was still rare (Fig. 3e). At P7, lamina propria and urothelial innervation were significantly higher than at P2, indicating a slower maturation than muscle nerves and a caudal increase in density (Fig. 3f–h).

Noradrenergic axons are much less prevalent than cholinergic axons in the adult rodent bladder; they form a sparse supply in the muscle (increasing in density at the bladder neck) and are sparse or absent near the urothelium; they also innervate the arterial vessels (Beckel and Holstege, 2011a; Forrest et al., 2014). Noradrenergic axons were identified by TH (tyrosine hydroxylase, *Th*) (Fig. 4a–f). At E13 we identified a sparse innervation of the outer bladder wall, most often found in the dorsal region (Fig. 4a). By E16, TH axons extended further around the circumference of the bladder, as previously identified by pan-neural mapping (Section 3.1). Muscle innervation was more pronounced near the neck of the bladder, and sparse noradrenergic axons were also associated with blood vessels within the muscle and the lamina propria. Noradrenergic innervation of the bladder muscle and vasculature continued to increase in density from E18 to P2 (Fig. 4b, d, e), with P7 appearing comparable to adult (Fig. 4c). Intramural micro-ganglia containing intensely TH-positive neurons were occasionally identified in sections from E16 to adulthood (Fig. 4f).

Many autonomic ganglion cells express NPY (neuropeptide Y, *Npy*). Although best characterised in sympathetic vasoconstrictor axons (Abe et al., 2007), in adult rodent pelvic ganglia NPY is expressed in both noradrenergic and a subclass of cholinergic neurons (Keast, 1995; Wanigasekara et al., 2003). We identified NPY axons in the developing and postnatal bladder (Fig. 4g–i), demonstrating similar principles of spatiotemporal patterning described for the cholinergic axon population, which forms the predominant subclass. At E18, a moderate density of axons was present in the dorsal muscle but less prevalent in the ventral region (Fig. 4g). By P2, muscle innervation had increased and lamina propria innervation was identified (Fig. 4h); the latter increased caudally, towards the bladder neck. Muscle and urothelial axons continued to increase in density between P2 and adulthood (Fig. 4i). In summary, patterning and density of NPY innervation resembled aspects of both noradrenergic innervation (vascular innervation) and cholinergic innervation (caudal gradient of urothelial innervation, with moderate to dense muscle innervation).

3.3 Development and maturation of sensory innervation of the bladder

Peptidergic sensory axons were identified by immunoreactivity for CGRP (calcitonin gene-related peptide, *Calca*; Fig. 5a–h, l–n) or SP (substance P, *Tac1*; Fig 5i, j). In adult rodents, peptidergic sensory axons are located in the muscle, where they form a plexus of lower density than cholinergic motor axons, and close to the urothelium, where they have an increasing density towards the bladder neck (Forrest et al., 2014; Gabella and Davis, 1998). Neither type of immunoreactivity was evident in the bladder at E13. At E16, CGRP axons formed a sparse plexus in the bladder muscle and lamina propria but did not yet reach the urothelium; in the muscle, innervation was more pronounced in the dorsal region (Fig. 5a, b). Despite this modest axon labelling in the bladder at E16, many CGRP neurons were identified in lumbosacral dorsal root ganglia (Fig. 5k). At E18, the innervation of both the muscle and lamina propria had increased slightly, but the urothelium remained without innervation (Fig. 5c, d). Further increases in innervation density occurred postnatally until P7 (Fig. 5e, f). Urothelial innervation was reliably identified by P2 and continued to increase in density to P7 and then further to adulthood (Fig. 5e–h); this showed a pronounced gradient of innervation, increasing towards the bladder neck and continuing to the proximal urethra. SP innervation showed a similar overall timeline and patterning of innervation but at each stage there were less axons visualised than with CGRP immunostaining (Fig.5 i, j). To compare the mature endpoint of sensory and autonomic innervation, we also performed double-labelling for VAChT and CGRP in the adult bladder (Fig. 5l–n). This demonstrated the distinct patterns of each axon class, the muscle having more prominent autonomic innervation, whereas the lamina propria and urothelium had more prominent sensory innervation.

A specific class of sensory axons in the bladder has nociceptive properties and is required for bladder-initiated pain (Franken et al., 2014; Grundy et al., 2019). These comprise a subgroup of peptidergic and non-peptidergic unmyelinated classes (Forrest et al., 2013) so their projections could not be inferred from our SP and CGRP results. Here we mapped the emergence and maturation of nociceptive innervation using a reporter mouse that reliably indicates Trpv1 expression (Cavanaugh et al., 2011), as TRPV1 antibodies do not reliably identify the complete terminal fields and many demonstrate specificity limitations

(Everaerts et al., 2009). Using alkaline phosphatase histochemistry to reveal structures expressing TRPV1 (Fig. 6), we identified neurons in embryonic dorsal root ganglia and their projections to the spinal cord dorsal horn (Fig. 6a, c). TRPV1 nociceptive axons followed a similar pattern and timing of development as CGRP and SP axons, being visible from E16 (Fig. 6b), increasing in density at E18 and further at P2 (Fig. 6e), reaching maximum density postnatally. A similar dorsoventral gradient of innervation was observed during this period, with muscle innervation proceeding earlier than lamina propria and urothelial innervation. To validate our non-immunohistochemical methodology as being sufficiently sensitive to demonstrate the complete terminal field of nociceptive axons, we performed labelling of the entire wall thickness, visualised in whole mounts (Fig. 6f).

3.4 Structural and molecular changes in the PG during the period of bladder innervation

Here we focused on the functional neural classifiers that we previously identified within the developing and/or mature bladder. This approach provided the opportunity to identify autonomic ganglion neurons relevant to bladder function prior to three fundamental events that define their functional regulation of bladder tissues: (1) defasciculation of axon bundles into individual axons; (2) extension of axons throughout the complete muscle layer; and (3) connectivity with axon terminals that originate from spinal preganglionic neurons, activity of which drives the motor responses in bladder tissues.

The bilateral PG are closely embedded between the urogenital organs so change in shape and proximity to the lower urinary tract as the reproductive organs mature (Georgas et al., 2015; Wiese et al., 2017; Yan and Keast, 2008). Here we identified PG in both coronal (Fig. 7a–d) and sagittal (Fig. 7e) sections through the embryo. Noradrenergic (TH) cells were identified in PG from E12, with many showing bright or moderate immunoreactivity (Fig. 8a, b). VAChT immunoreactivity was also present but it was more difficult to distinguish positive from negative cells; this was also the case for more mature PG neurons (see below) and is a limitation of visualising cholinergic neurons by the location of a transporter protein that is preferentially co-located with transmitter release, at axon terminals. In E13 embryo sections we also noted bright TH immunolabeling in pre- and paravertebral sympathetic ganglia but weak TH immunolabeling in dorsal root ganglia, an additional source of catecholamine-synthesizing axons in adult mice (Brumovsky et al., 2012; Meerschaert et al., 2020; Usoskin et al., 2015).

VAChT immunolabeling also demonstrated bright puncta surrounding the developing PG neurons (Fig. 8a, c, d). These structures, characteristic of terminals originating from spinal preganglionic neurons (Keast, 1995) became more prevalent from E12 to E18. This indicates that structural connectivity of the circuit commenced prior to innervation of the bladder tissues and continued to mature during this process.

We then examined other neurally expressed genes that had earlier undergone intramural mapping within axons of the bladder. Although nNOS axons were undetectable in the bladder at E13, many nNOS neurons were evident in the PG at this time (Fig. 8e). At E16, a stage at which nNOS axons were still quite sparsely distributed in the bladder (Fig. 3b), brightly labelled nNOS neurons were common (Fig. 8f); nNOS neurons continued to be a major population of PG neurons from E18 to the postnatal period (Fig. 8g–i). In contrast,

only a very small population of PG neurons was NPY-immunoreactive prior to birth (Fig. 8j, k), but many NPY neurons were present postnatally (Fig. 8l).

Analysis of putative sensory markers, SP and CGRP, was predicted to demonstrate axons passing through the PG en route to pelvic organs and potentially their axon collaterals which, in adult rats, are associated with PG neurons that project to the lower urinary tract (Bertrand et al., 2020). We prioritised our analysis to CGRP, which from E16 identified a greater number of axons in the muscle and lamina propria than SP. Unexpectedly, we identified numerous, brightly immunolabelled CGRP-positive neuronal cell bodies in PG from both male and female embryos. These were identified at E14 (Fig. 9a; earlier stages not examined), were prevalent from E16-E18 (Fig. 9c–e) and were scarce postnatally; we were unable to identify CGRP cell bodies in the PG from P7. CGRP boutons were associated with many PG neurons from E18 (Fig. 9c). We performed a more targeted analysis of SP in PG and found no evidence of SP-positive neuronal cell bodies prior to birth (Fig. 9a, d). At E18 we identified numerous SP axons that formed boutons in close association with unlabelled PG neurons (Fig. 9d).

We then considered that this transient expression of CGRP by PG neurons had the potential to confound our functional interpretation of CGRP axons within the bladder wall, so examined the potential colocalization of CGRP and VAChT within bladder axons at times when they were highly coexpressed in PG cell bodies. While we were able to visualise a very small population of axons that labelled for both markers, from E16 to P7 the majority of CGRP and VAChT immunolabelling occurred in distinct axon populations (Fig. 9f), indicating that CGRP-positive PG neurons did not transport detectable amounts of CGRP to their axon terminals and that our earlier mapping did indeed primarily visualise sensory axons. During the course of this analysis, we frequently identified CGRP and VAChT axons that were very closely apposed and intertwined (long arrow, Fig. 9f), as observed in adult bladder (Fig. 5l–n). These close sensory-motor associations were evident in the muscle and lamina propria, including the suburothelial tissues, from E16.

Discussion

In this study, we found that innervation of the urinary bladder commenced at E13 and progressively increased in density towards its mature structural form throughout embryonic development, only achieving the full complement of terminal fields in the postnatal period. The spatiotemporal patterning of each nerve class is summarised for each tissue in Figure 10. Across all nerve classes, innervation extended dorsoventrally across the bladder wall, commencing prior to the maturation of smooth muscle in the detrusor. Smooth muscle cells detectable by their *Acta2* expression are present in the primitive bladder at E13 but do not form a distinctive compact layer (detrusor) at that time (Carpenter et al., 2012; Georgas et al., 2015). Furthermore, muscle maturation proceeds from the distal fundus (apex) towards the bladder neck (Carpenter et al., 2012; Wiese et al., 2017), which differs from the innervation gradient (apex is innervated later than the bladder neck).

This spatial patterning of axonal defasciculation and extension demonstrated a more subtle dorsoventral patterning in the lamina propria and urothelium, where a more obvious

regionalisation occurred in the rostrocaudal direction. Here, all axon classes innervating the urothelium showed a graded increase of density towards the bladder neck. This gradient became evident prior to birth and was further enhanced in the postnatal period. Together, this regionality raises interesting questions of the mechanisms driving growth of axon tracts and expansion of terminal fields into specific tissues and tailored to individual nerve classes. This is relevant not only to understanding issues arising from impaired development of urogenital regulation but also to restoration of function following injury to the adult neural projections, which are vulnerable during pelvic surgery. Strategies to establish appropriate innervation patterns within the bladder is also an important component of regenerative medicine approaches that will need to provide not only a broadly supportive environment for neural pathways but ensure their correct connectivity with specific tissue types.

Although several broad principles of axonal patterning were common across functional nerve classes, each had a distinct timing for achieving maximum innervation and distribution across tissue classes (detrusor muscle, vascular, lamina propria/urothelium). These distinguishing features could potentially be driven by temporal and spatial differences in the expression of growth and guidance factors within tissues and regions of the bladder wall, or the expression of relevant receptors within specific periods of development of bladder-projecting sensory and autonomic neurons. Several families of neurotrophic factor receptors have been mapped or implicated in function of relevant populations of sensory and autonomic neurons (Ernsberger, 2008; Ernsberger et al., 2020; Forrest et al., 2013; Golden et al., 2010; Hoshi et al., 2012; Keast et al., 2015) but the approaches used to date have not distinguished neurons projecting to different regions or tissues within the bladder. Much also remains to be learned about neural guidance factors and other potential directional and neurotrophic mechanisms in the pelvic viscera. Understanding these mechanisms is of particular interest for the bladder neck, a region that shows the highest density of two axon classes: peptidergic sensory axons innervating the urothelium and the nitrergic subclass of cholinergic axons innervating the muscle wall. Neuro-urothelial communication has been strongly implicated in numerous bladder functions and clinical conditions (Birder and Andersson, 2013) and the inhibitory role of nitrergic transmission in the bladder neck is relevant to conditions to improve efficiency of voiding and improvement of continence (Andersson, 1993; Andersson, 2016). Our study showed that urothelial innervation was absent or sparse during the embryonic period when the urothelium is undergoing its primary differentiation into cellular subtypes (Georgas et al., 2015; Wang et al., 2017), with substantial expansion of urothelial innervation after birth. It would be of interest to determine if postnatal changes in expression of urothelium-derived factors drive this increased innervation.

To interpret our studies in the broader context of organ regulation, it will also be important to define the capacity for these developing terminal fields to communicate with specific tissues in the bladder. This includes defining sensory and motor activity, synaptic function and smooth muscle transduction mechanisms in the embryo and the postnatal period. Numerous studies across several species indicate that axons in the bladder muscle and components of related central circuits continue to mature functionally in the postnatal period (de Groat and Yoshimura, 2015; Dutton et al., 1999; Kruse and de Groat, 1993; Levin et al., 1981; Longhurst, 2004; Maggi et al., 1988; Maggi et al., 1984, 1986; Oh et al., 2000; Pirker

et al., 2005; Sneddon and McLees, 1992; Szell et al., 2003; Thor et al., 1990), however the functionality of these synapses prior to birth remains, to our knowledge, unexplored. The majority of physiology research focused on immature neural circuitry relating to the bladder has been performed on postnatal rats, with very little investigation of the embryonic period in any species. Likewise, the emergence of transduction properties in bladder sensory pathways remains relatively poorly understood. Fundamental aspects of sensory neuron lineages, such as emergence of primary functional subclasses defined by transient receptor potential (TRP) channels, have been characterised in the total population of dorsal root ganglion neurons (Hjerling-Leffler et al., 2007), but to our knowledge have not been defined specifically in developing visceral afferents. At maturity, visceral afferents demonstrate many features distinct from somatic afferents (Gebhart and Bielefeldt, 2016; Grundy et al., 2019; Meerschaert et al., 2020; Smith-Anttila et al., 2020), but these have not yet been explored across during the period of embryonic development when their peripheral terminal fields are being established. Likewise, their central terminal fields in the sacral cord have been demonstrated from E16 (Funakoshi et al., 2003; Funakoshi et al., 2006), but their function at this time is unknown.

Our studies of pelvic ganglia demonstrated several important concepts of circuit formation and function in this region. The presence of cholinergic boutons in the pelvic ganglion preceded innervation of the bladder tissue. Although we did not have tools to specifically distinguish bladder-projecting pelvic ganglion neurons in our study, the putative cholinergic inputs we observed at E12 cannot be explained by neural circuits regulating other pelvic organs being more mature, as other pelvic organs also only begin to be innervated from E13-E14 (Erickson et al., 2012; Niu et al., 2020; Turco et al., 2019; Yan and Keast, 2008). Our observations build upon the report that spinal nerve tracts reach the primordial pelvic ganglion at E11.5 and merge with the ganglion at E13.5 (Espinosa-Medina et al., 2016). We did not perform ultrastructural or electrophysiological studies on the immature pelvic ganglion to determine when these boutons formed mature synapses, but our observations provide compelling evidence for spinal cord to ganglion connectivity to begin well prior to ganglion connectivity with the lower urinary tract; this contrasts with several other regions of the autonomic nervous system (Glebova and Ginty, 2005). This in turn suggests that initial construction of this circuit does not require organ-derived molecular or electrical signals.

The pelvic ganglion is an unusually complex region of the autonomic nervous system where two of the major components of the autonomic system (sympathetic and parasympathetic) are intermingled (Ernsberger et al., 2020; Keast, 1999, 2006), rather than being organised as separate sympathetic and parasympathetic ganglia. To interpret our new data in the context of the broader literature, it is important to define the terms “sympathetic” and “parasympathetic” as they can be misunderstood. The most robust and broadly accepted definition of these terms is based on anatomy of neuronal circuits within the adult, in which the location of the premotor (i.e., preganglionic) CNS neuron defines the classifier applied to the pathway (Horn, 2018). This principle is easily applied to the pelvic ganglion, where neurons innervated by preganglionic neurons in the thoracolumbar cord are classified as sympathetic and those innervated by sacral preganglionic neurons are parasympathetic. This clear distinction also reflects the quite different properties of sympathetic and

parasympathetic pathways, especially their distinct connectivity to brain regions and activity patterns that define their adult function. In our study, we deliberately avoided the terms sympathetic and parasympathetic as our experiments did not define the source of the spinal inputs to PG neurons. Although we can likely infer that all of the TH neurons were sympathetic (because in the adult all of these neurons receive synaptic inputs from lumbar preganglionic neurons), we could not classify the other neuron classes (VAChT, nNOS, NPY), which in adults are divided into sympathetic and parasympathetic classes, based on their origins of spinal input (Keast, 1995). There is currently insufficient information available on developing preganglionic neurons to further classify these classes of embryonic or postnatal pelvic ganglion neurons.

An unexpected aspect of our pelvic ganglion characterization was the transient expression of CGRP, generally viewed as reliable peptide marker of a major class of visceral afferents (Gebhart and Bielefeldt, 2016; Grundy et al., 2019). We found that until E18 CGRP was prevalent in pelvic ganglion neurons, but we did not further classify the CGRP neurons as noradrenergic or cholinergic. Irrespective, it was difficult to detect CGRP labelling in cholinergic axons within the embryonic bladder, suggesting that these CGRP-expressing pelvic ganglion neurons did not transport CGRP to their axon terminals. This fortuitous observation allowed us to infer that our earlier mapping of CGRP axons in the developing bladder was likely representative of sensory patterning. It would be of interest to define the function of this transient CGRP expression by pelvic ganglion neurons, especially to determine if it may play a role in defining aspects of preganglionic or organ connectivity and function.

Several technical aspects of our study warrant further consideration. First, relating to functional classification, we have relied primarily on major adult neuronal phenotypes to attribute classifications to nNOS and TH axons in the embryo. The strong expression of nNOS in developing and pelvic ganglia provides support for our classification of nNOS axons as cholinergic autonomic, however, we cannot discount that a minority may be sensory (Forrest et al., 2013; Vizzard et al., 1995). Likewise, while TH immunohistochemistry will reliably label noradrenergic neurons in pelvic ganglia, it is possible that some TH axons in the developing bladder originate from dorsal root ganglia (Brumovsky et al., 2012; Meerschaert et al., 2020). We have not ruled out this possibility but consider this at most a minor contributor, given the low level of TH expression within sensory ganglia prior to birth. Second, our study relied on careful observation of technical and biological replicates, sampled in transverse and sagittal orientation, but did not quantify axon density or count pelvic ganglion neurons. Therefore, it is possible that we failed to identify more subtle changes in axon density or sexual dimorphisms. Pelvic ganglia are known to be sexually dimorphic, containing more neurons and a higher proportion of noradrenergic neurons in adult rodents (Greenwood et al., 1985; Melvin and Hamill, 1987, 1989; Melvin et al., 1989; Suzuki et al., 1982). The age at which this dimorphism is established is not known, but is largely attributed to the reproductive organs receiving a stronger innervation in males than females (Keast, 2006). Our assessment of pelvic ganglia did not include quantitation or strategies such as serially sectioning to allow this level of assessment. The development of large volume clearing and immunolabeling methods will provide an excellent opportunity for detailed analysis of this type.

Conclusions

These studies have enhanced our understanding of neural regulatory elements in the lower urinary tract during development and provide a foundation for studies of plasticity and regenerative capacity in the adult system.

Acknowledgments

Ms Elsy Richardson assisted with tissue processing and microscopy of embryonic bladders. Dr Adam Wallace participated in early embryo data collection and image upload to GUDMAP.

Funding sources

This study was supported by the US National Institutes of Health (1U01DK101029, 5UO1DK094479; JRK).

References

Abe K, Tilan JU, Zukowska Z, 2007. NPY and NPY receptors in vascular remodeling. Curr Top Med Chem 7, 1704–1709. [PubMed: 17979779]

Anderson RB, Stewart AL, Young HM, 2006. Phenotypes of neural-crest-derived cells in vagal and sacral pathways. Cell Tissue Res 323, 11–25. [PubMed: 16133146]

Andersson K-E, 1993. Pharmacology of lower urinary tract smooth muscles and penile erectile tissues. Pharmacol. Rev 45, 253–308. [PubMed: 8248281]

Andersson KE, 2016. Potential future pharmacological treatment of bladder dysfunction. Basic Clin Pharmacol Toxicol 119 Suppl 3, 75–85. [PubMed: 26990140]

Beckel JM, Holstege G, 2011a. Neuroanatomy of the lower urinary tract. Handb Exp Pharmacol, 99–116. [PubMed: 21290224]

Beckel JM, Holstege G, 2011b. Neurophysiology of the lower urinary tract. Handb Exp Pharmacol, 149–169.

Bertrand MM, Korajkic N, Osborne PB, Keast JR, 2020. Functional segregation within the pelvic nerve of male rats: a meso- and microscopic analysis. J Anat 237, 757–773. [PubMed: 32598494]

Birder L, Andersson KE, 2013. Urothelial signaling. Physiol Rev 93, 653–680. [PubMed: 23589830]

Brumovsky PR, La JH, McCarthy CJ, Hokfelt T, Gebhart GF, 2012. Dorsal root ganglion neurons innervating pelvic organs in the mouse express tyrosine hydroxylase. Neuroscience 223, 77–91. [PubMed: 22858598]

Carpenter A, Paulus A, Robinson M, Bates CM, Robinson ML, Hains D, Kline D, McHugh KM, 2012. 3-Dimensional morphometric analysis of murine bladder development and dysmorphogenesis. Dev Dyn 241, 522–533. [PubMed: 22275180]

Cavanaugh DJ, Chesler AT, Jackson AC, Sigal YM, Yamanaka H, Grant R, O'Donnell D, Nicoll RA, Shah NM, Julius D, Basbaum AI, 2011. Trpv1 reporter mice reveal highly restricted brain distribution and functional expression in arteriolar smooth muscle cells. J Neurosci 31, 5067–5077. [PubMed: 21451044]

de Groat WC, Yoshimura N, 2015. Anatomy and physiology of the lower urinary tract. Handb Clin Neurol 130, 61–108. [PubMed: 26003239]

Dickson A, Avelino A, Cruz F, Ribeiro-da-Silva A, 2006. Peptidergic sensory and parasympathetic fiber sprouting in the mucosa of the rat urinary bladder in a chronic model of cyclophosphamide-induced cystitis. Neuroscience 141, 1633–1647. [PubMed: 16989017]

Dutton JL, Hansen MA, Balcar VJ, Barden JA, Bennett MR, 1999. Development of P2X receptor clusters on smooth muscle cells in relation to nerve varicosities in the rat urinary bladder. J Neurocytol 28, 4–16. [PubMed: 10573604]

Erickson CS, Zaitoun I, Haberman KM, Gosain A, Druckenbrod NR, Epstein ML, 2012. Sacral neural crest-derived cells enter the aganglionic colon of Ednrb−/− mice along extrinsic nerve fibers. J Comp Neurol 520, 620–632. [PubMed: 21858821]

Ernsberger U, 2008. The role of GDNF family ligand signalling in the differentiation of sympathetic and dorsal root ganglion neurons. Cell Tissue Res 333, 353–371. [PubMed: 18629541]

Ernsberger U, Deller T, Rohrer H, 2020. The diversity of neuronal phenotypes in rodent and human autonomic ganglia. Cell Tissue Res 382, 201–231. [PubMed: 32930881]

Espinosa-Medina I, Saha O, Boismoreau F, Chettouh Z, Rossi F, Richardson WD, Brunet JF, 2016. The sacral autonomic outflow is sympathetic. Science 354, 893–897. [PubMed: 27856909]

Everaerts W, Sepulveda MR, Gevaert T, Roskams T, Nilius B, De Ridder D, 2009. Where is TRPV1 expressed in the bladder, do we see the real channel? Naunyn Schmiedebergs Arch Pharmacol 379, 421–425. [PubMed: 19153713]

Forrest SL, Osborne PB, Keast JR, 2013. Characterization of bladder sensory neurons in the context of myelination, receptors for pain modulators, and acute responses to bladder inflammation. Front Neurosci 7, 206. [PubMed: 24223534]

Forrest SL, Osborne PB, Keast JR, 2014. Characterization of axons expressing the artemin receptor in the female rat urinary bladder: a comparison with other major neuronal populations. J Comp Neurol 522, 3900–3927. [PubMed: 25043933]

Franken J, Uvin P, De Ridder D, Voets T, 2014. TRP channels in lower urinary tract dysfunction. Br J Pharmacol 171, 2537–2551. [PubMed: 24895732]

Funakoshi K, Goris RC, Kadota T, Atobe Y, Nakano M, Kishida R, 2003. Prenatal development of peptidergic primary afferent projections to mouse lumbosacral autonomic preganglionic cell columns. Brain Res Dev Brain Res 144, 107–119. [PubMed: 12888222]

Funakoshi K, Nakano M, Atobe Y, Kadota T, Goris RC, 2006. Prenatal development of transient receptor potential vanilloid 1-expressing primary sensory projections to sacral autonomic preganglionic neurons. Neurosci Lett 407, 230–233. [PubMed: 16973277]

Gabella G, 1995. The structural relations between nerve fibres and muscle cells in the urinary bladder of the rat. J Neurocytol 24, 159–187. [PubMed: 7798112]

Gabella G, Davis C, 1998. Distribution of afferent axons in the bladder of rats. J Neurocytol 27, 141–155. [PubMed: 10640174]

Gebhart GF, Bielefeldt K, 2016. Physiology of visceral pain. Compr Physiol 6, 1609–1633. [PubMed: 27783853]

Georgas KM, Armstrong J, Keast JR, Larkins CE, McHugh KM, Southard-Smith EM, Cohn MJ, Batourina E, Dan H, Schneider K, Buehler DP, Wiese CB, Brennan J, Davies JA, Harding SD, Baldock RA, Little MH, Vezina CM, Mendelsohn C, 2015. An illustrated anatomical ontology of the developing mouse lower urogenital tract. Development 142, 1893–1908. [PubMed: 25968320]

Gillespie JI, Markerink-van Ittersum M, de Vente J, 2006. Sensory collaterals, intramural ganglia and motor nerves in the guinea-pig bladder: evidence for intramural neural circuits. Cell Tissue Res 325, 33–45. [PubMed: 16525831]

Glebova NO, Ginty DD, 2005. Growth and survival signals controlling sympathetic nervous system development. Annu Rev Neurosci 28, 191–222. [PubMed: 16022594]

Golden JP, Hoshi M, Nassar MA, Enomoto H, Wood JN, Milbrandt J, Gereau R.W.t., Johnson EM Jr., Jain S, 2010. RET signaling is required for survival and normal function of nonpeptidergic nociceptors. J Neurosci 30, 3983–3994. [PubMed: 20237269]

Gonzalez EJ, Merrill L, Vizzard MA, 2014. Bladder sensory physiology: neuroactive compounds and receptors, sensory transducers, and target-derived growth factors as targets to improve function. Am J Physiol Regul Integr Comp Physiol 306, R869–878. [PubMed: 24760999]

Greenwood D, Coggeshall RE, Hulsebosch CE, 1985. Sexual dimorphism in the numbers of neurons in the pelvic ganglia of adult rats. Brain Res 340, 160–162. [PubMed: 4027642]

Grundy L, Erickson A, Brierley SM, 2019. Visceral pain. Annu Rev Physiol 81, 261–284. [PubMed: 30379615]

Hjerling-Leffler J, Alqatari M, Ernfors P, Koltzenburg M, 2007. Emergence of functional sensory subtypes as defined by transient receptor potential channel expression. J Neurosci 27, 2435–2443. [PubMed: 17344381]

Horn JP, 2018. The sacral autonomic outflow is parasympathetic: Langley got it right. Clin Auton Res 28, 181–185. [PubMed: 29453697]

Hoshi M, Batourina E, Mendelsohn C, Jain S, 2012. Novel mechanisms of early upper and lower urinary tract patterning regulated by RetY1015 docking tyrosine in mice. Development 139, 2405–2415. [PubMed: 22627285]

Keast JR, 1995. Visualization and immunohistochemical characterization of sympathetic and parasympathetic neurons in the male rat major pelvic ganglion. Neuroscience 66, 655–662. [PubMed: 7644029]

Keast JR, 1999. Unusual autonomic ganglia: connections, chemistry, and plasticity of pelvic ganglia. Int Rev Cytol 193, 1–69. [PubMed: 10494620]

Keast JR, 2006. Plasticity of pelvic autonomic ganglia and urogenital innervation. Int Rev Cytol 248, 141–208. [PubMed: 16487791]

Keast JR, Smith-Anttila CJ, Osborne PB, 2015. Developing a functional urinary bladder: a neuronal context. Front Cell Dev Biol 3, 53. [PubMed: 26389118]

Kruse MN, de Groat WC, 1993. Spinal pathways mediate coordinated bladder/urethral sphincter activity during reflex micturition in decerebrate and spinalized neonatal rats. Neurosci Lett 152, 141–144. [PubMed: 8515867]

Levin RM, Malkowicz SB, Jacobowitz D, Wein AJ, 1981. The ontogeny of the autonomic innervation and contractile response of the rabbit urinary bladder. J Pharmacol Exp Ther 219, 250–257. [PubMed: 7288610]

Longhurst P, 2004. Developmental aspects of bladder function. Scand J Urol Nephrol Suppl, 11–19. [PubMed: 15545192]

Maggi CA, Santicioli P, Geppetti P, Frilli S, Spillantini MG, Nediani C, Hunt SP, Meli A, 1988. Biochemical, anatomical and functional correlates of postnatal development of the capsaicin-sensitive innervation of the rat urinary bladder. Brain Res 471, 183–190. [PubMed: 2460197]

Maggi CA, Santicioli P, Meli A, 1984. Postnatal development of myogenic contractile activity and excitatory innervation of rat urinary bladder. Am J Physiol 247, R972–978. [PubMed: 6150648]

Maggi CA, Santicioli P, Meli A, 1986. Postnatal development of micturition reflex in rats. Am J Physiol 250, R926–931. [PubMed: 3706578]

Meerschaert KA, Adelman PC, Friedman RL, Albers KM, Koerber HR, Davis BM, 2020. Unique molecular characteristics of visceral afferents arising from different levels of the neuraxis: location of afferent somata predicts function and stimulus detection modalities. J Neurosci 40, 7216–7228. [PubMed: 32817244]

Melvin JE, Hamill RW, 1987. The major pelvic ganglion: androgen control of postnatal development. J Neurosci 7, 1607–1612. [PubMed: 3598637]

Melvin JE, Hamill RW, 1989. Androgen-specific critical periods for the organization of the major pelvic ganglion. J Neurosci 9, 736–742. [PubMed: 2918385]

Melvin JE, McNeill TH, Hervonen A, Hamill RW, 1989. Organizational role of testosterone on the biochemical and morphological development of the hypogastric ganglion. Brain Res 485, 1–10. [PubMed: 2566358]

Niu X, Liu L, Wang T, Chuan X, Yu Q, Du M, Gu Y, Wang L, 2020. Mapping of extrinsic innervation of the gastrointestinal tract in the mouse embryo. J Neurosci 40, 6691–6708. [PubMed: 32690615]

Oh SJ, Lee KH, Kim SJ, Kim KW, Kim KM, Choi H, 2000. Active properties of the urinary bladder: in vitro comparative studies between adult and neonatal rats. BJU Int 85, 1126–1133. [PubMed: 10848709]

Pirker ME, Montedonico S, Rolle U, Austvoll H, Puri P, 2005. Regional differences in nitrergic neuronal density in the developing porcine urinary bladder. Pediatr Surg Int 21, 161–168. [PubMed: 15570429]

Smith-Anttila CJA, Mason EA, Wells CA, Aronow BJ, Osborne PB, Keast JR, 2020. Identification of a sacral, visceral sensory transcriptome in embryonic and adult mice. eNeuro 7.

Sneddon P, McLees A, 1992. Purinergic and cholinergic contractions in adult and neonatal rabbit bladder. Eur J Pharmacol 214, 7–12. [PubMed: 1582452]

Suzuki Y, Ishii H, Furuya H, Arai Y, 1982. Developmental changes of the hypogastric ganglion associated with the differentiation of the reproductive tracts in the mouse. Neurosci Lett 32, 271–276. [PubMed: 7177491]

Szell EA, Somogyi GT, de Groat WC, Szigeti GP, 2003. Developmental changes in spontaneous smooth muscle activity in the neonatal rat urinary bladder. Am J Physiol Regul Integr Comp Physiol 285, R809–816. [PubMed: 12750150]

Thor KB, Blais DP, Kawatani M, Erdman S, de Groat WC, 1990. Postnatal development of opioid regulation of micturition in the kitten. Brain Res Dev Brain Res 57, 255–261. [PubMed: 1705869]

Turco AE, Cadena MT, Zhang HL, Sandhu JK, Oakes SR, Chathurvedula T, Peterson RE, Keast JR, Vezina CM, 2019. A temporal and spatial map of axons in developing mouse prostate. Histochem Cell Biol 152, 35–45. [PubMed: 30976911]

Uesaka T, Young HM, Pachnis V, Enomoto H, 2016. Development of the intrinsic and extrinsic innervation of the gut. Dev Biol 417, 158–167. [PubMed: 27112528]

Usoskin D, Furlan A, Islam S, Abdo H, Lonnerberg P, Lou D, Hjerling-Leffler J, Haeggstrom J, Kharchenko O, Kharchenko PV, Linnarsson S, Ernfors P, 2015. Unbiased classification of sensory neuron types by large-scale single-cell RNA sequencing. Nat Neurosci 18, 145–153. [PubMed: 25420068]

Vizzard MA, Erdman SL, de Groat WC, 1995. Increased expression of neuronal nitric oxide synthase (NOS) in visceral neurons after nerve injury. J Neurosci 15, 4033–4045. [PubMed: 7538569]

Wang C, Ross WT, Mysorekar IU, 2017. Urothelial generation and regeneration in development, injury, and cancer. Dev Dyn 246, 336–343. [PubMed: 28109014]

Wanigasekara Y, Kepper ME, Keast JR, 2003. Immunohistochemical characterisation of pelvic autonomic ganglia in male mice. Cell Tissue Res 311, 175–185. [PubMed: 12596037]

Wiese CB, Deal KK, Ireland SJ, Cantrell VA, Southard-Smith EM, 2017. Migration pathways of sacral neural crest during development of lower urogenital tract innervation. Dev Biol 429, 356–369. [PubMed: 28449850]

Wiese CB, Ireland S, Fleming NL, Yu J, Valerius MT, Georgas K, Chiu HS, Brennan J, Armstrong J, Little MH, McMahon AP, Southard-Smith EM, 2012. A genome-wide screen to identify transcription factors expressed in pelvic ganglia of the lower urinary tract. Front Neurosci 6, 130. [PubMed: 22988430]

Yan H, Keast JR, 2008. Neurturin regulates postnatal differentiation of parasympathetic pelvic ganglion neurons, initial axonal projections, and maintenance of terminal fields in male urogenital organs. J Comp Neurol 507, 1169–1183. [PubMed: 18175352]

Highlights

- Sensory and motor axons project to the bladder tissues from E13 and continue to mature towards their adult patterning in the first postnatal week.
- Functionally distinct classes of axons achieved their adult patterning and density at different times.
- Urothelial innervation occurred more slowly than muscle innervation.
- Pelvic ganglion neurons receive spinal cholinergic inputs prior to the innervation of bladder tissues.

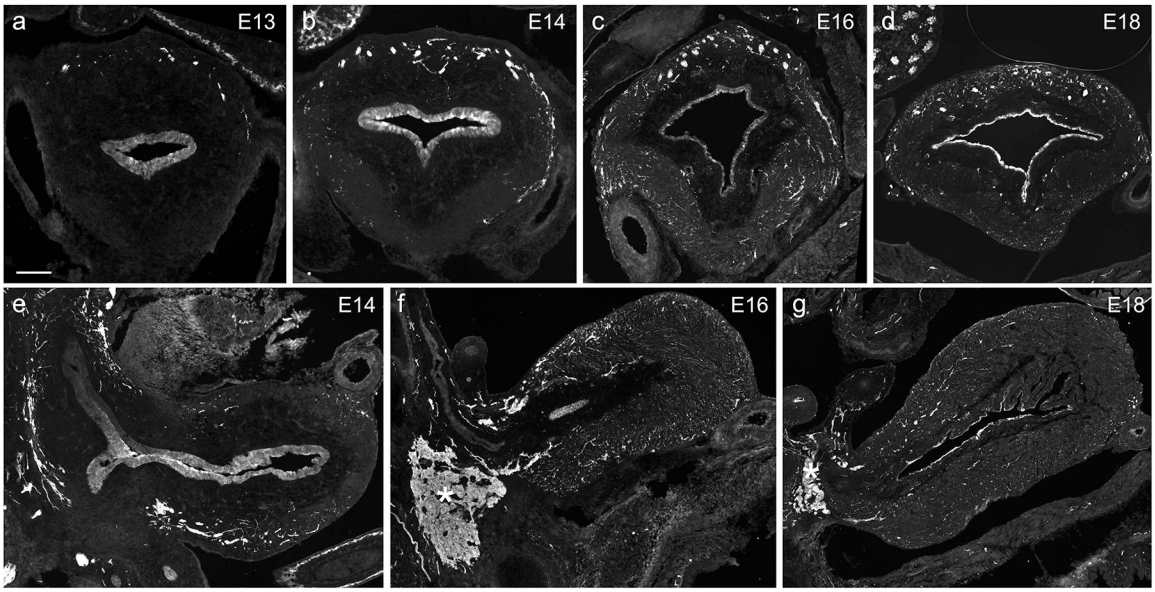

Figure 1: Mapping the total population of bladder axons in the mouse embryo.

Pan-neural labelling (PGP; protein gene product 9.5) in male embryos shows progressive innervation of the bladder wall from serosal to luminal surface, with the dorsal region being innervated prior to the ventral region. PGP immunoreactivity was also present in the urothelium. Panels **a-d** show transverse sections through the bladder body from E13-E18; images oriented with dorsal at the top. Panels **e-g** show the bladder and proximal urethra in sagittal sections; images are oriented with dorsal towards the bottom. The sections from E16 and E18 embryos also show aggregates of pelvic ganglion neurons (asterisk). Calibration: a 100 μm; b 120 μm; c, e 150 μm; d, f 200 μm; g 300 μm.

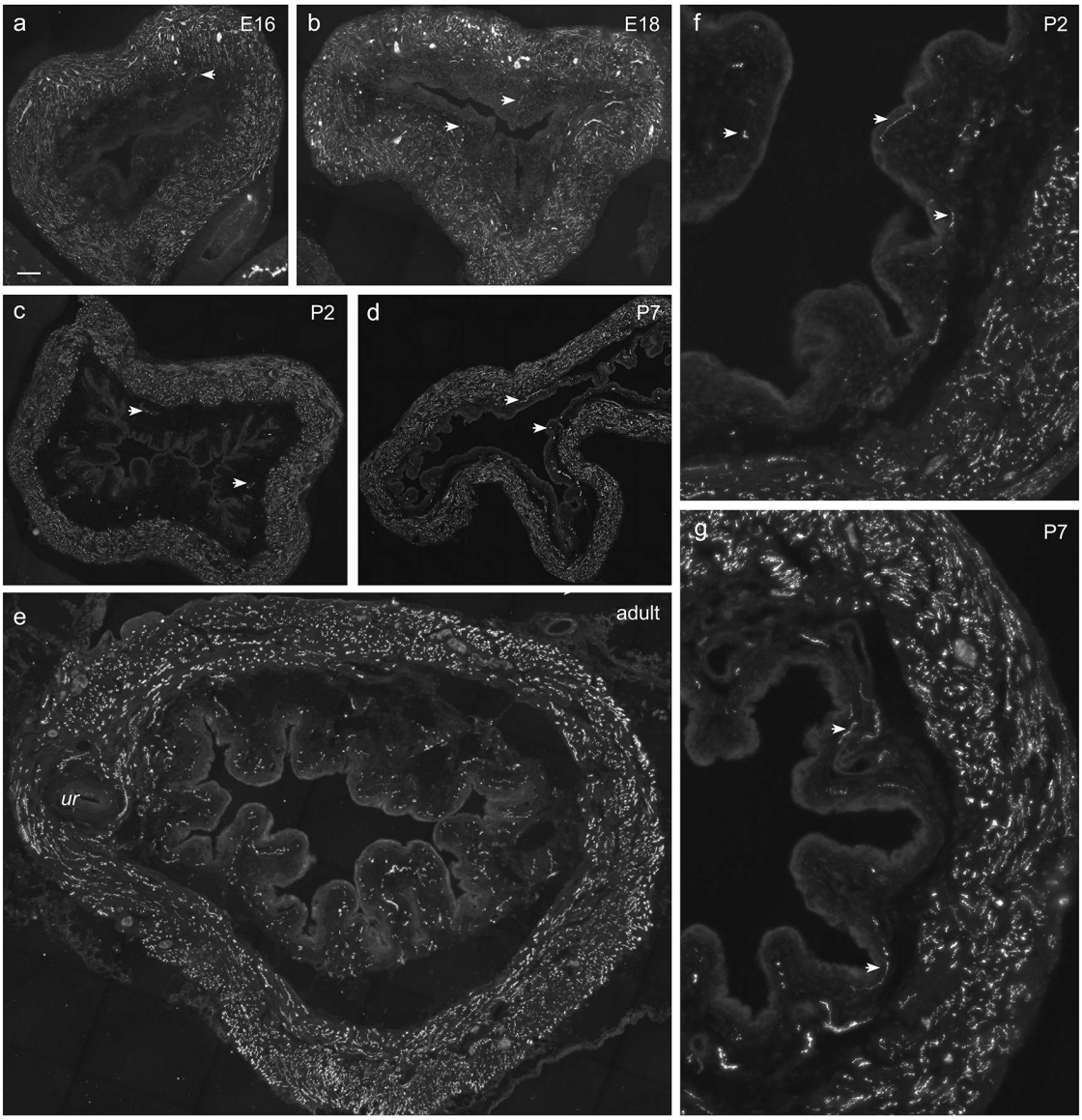

Figure 2: Cholinergic autonomic innervation of mouse urinary bladder in the pre- and postnatal periods.

Cholinergic axons are visualised by immunoreactivity to vesicular acetylcholine transporter (VAChT). All images are from bladder sectioned transversely. In panels **a-e**, images are oriented with dorsal to the top. **a**, E16 female; **b**, E18, female; **c**, P2 male; **d**, P7 male; **e**, adult female. A moderate (E16) to high (E18 onwards) density of cholinergic axons are present in the muscle but in the lamina propria cholinergic axons are scarce prior to birth (examples shown by arrows). The image of the adult bladder (**e)** is from a section at the level of the ureter entry shown on one side (*ur*). Higher magnification images (**f**, P2 male; **g**, P7 male) show the postnatal innervation of the lamina propria near the bladder neck; many of these axons lie very close to the urothelium (examples shown by arrows). Calibration: a, e 100 μm; b 75 μm; c 150 μm; d 200 μm; f, g 40 μm.

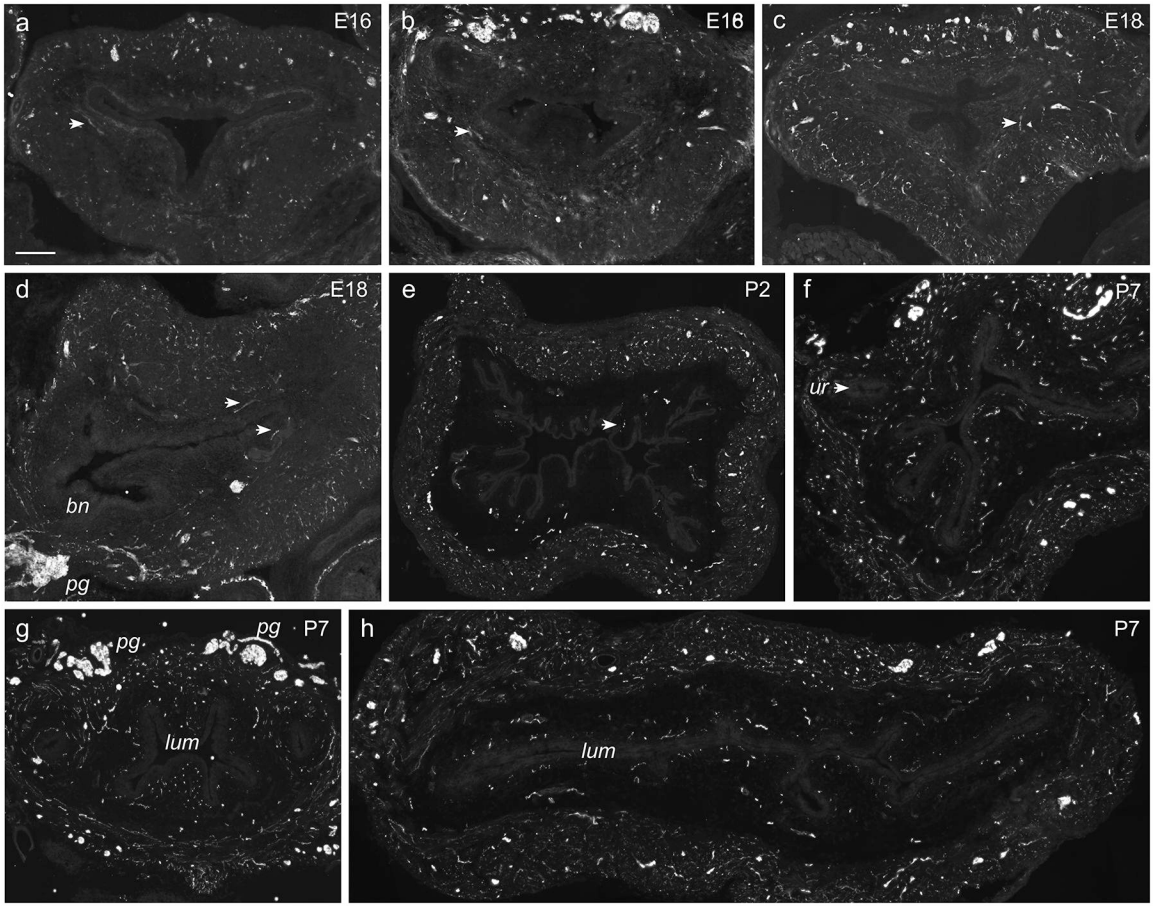

Figure 3: Nitrergic innervation of mouse urinary bladder in the pre- and postnatal periods.

Nitrergic axons are identified by immunoreactivity for neuronal nitric oxide synthase (nNOS). All panels are from bladder sectioned transversely and oriented with dorsal to the top, with the exception of **d** (sagittal, dorsal towards the bottom of the image). A moderate (E16) to high (E18 onwards) density of nitrergic axons is present in the muscle, but in the lamina propria nitrergic axons are scarce prior to birth (examples shown by arrows). **a, b**: E16, female, showing sections from the middle of the bladder (**a**) and closer to the bladder neck (**b**), with a progressive increase in axon density in the muscle towards the bladder neck. **c, d**: E18, male: nitrergic innervation comparable to the female at this stage of development, shown in transverse section near the bladder neck (**c**) and sagittal section (**d**). A part of the pelvic ganglion (*pg*) on one side is shown near the bladder neck (*bn*). **e-h**, show increasing innervation of the muscle and lamina propria in the postnatal period; **e**, P2 male; **f, g**, P7 male; **h**, P7, female. Lamina propria innervation has the highest density near the bladder neck, demonstrated in **f** (entry of ureter shown, *ur*) and **g** (transition to the urethra, showing adjacent pelvic ganglia, *pg*, and urethra lumen, *lum*). The lumen of the bladder in P7 bladder is also indicated (*lum*). Calibration: a-d, f, h 100 μm; g 120 μm, e, 150 μm.

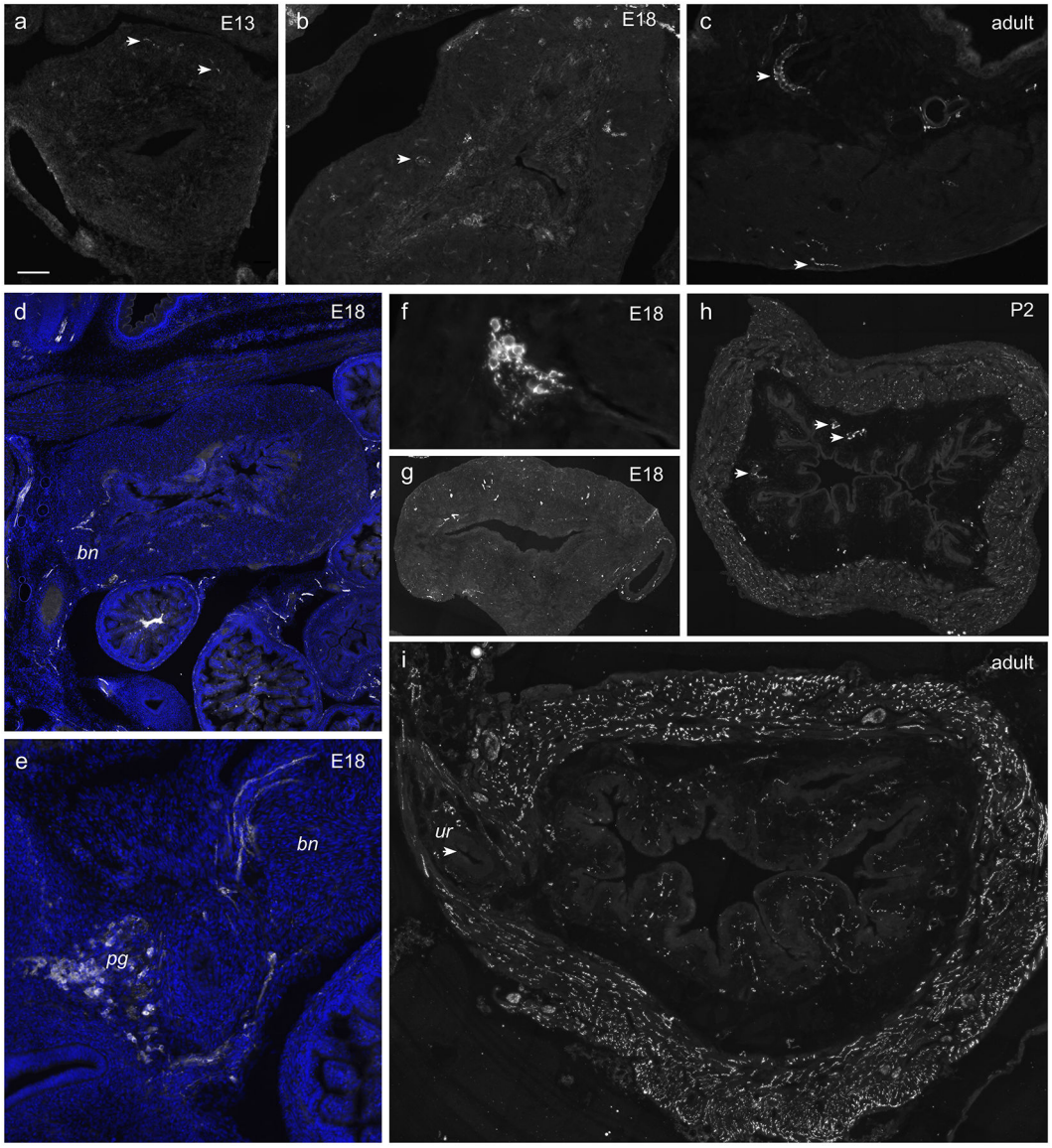

Figure 4: Noradrenergic and neuropeptide Y (NPY) autonomic innervation of the mouse urinary bladder in the pre- and postnatal periods.

Noradrenergic neural structures identified by immunoreactivity for TH (tyrosine hydroxylase) are shown in panels **a-f**, whereas axons immunolabelled for NPY (neuropeptide Y) are shown in panels g-**i**. Panels **a, c, f-I** are from bladder sectioned transversely and oriented with dorsal to the top, whereas panels **b, d** and **e** are from sagittal sections. **a**, E13 embryo shows rare TH axons (arrows). These are still sparse at E18 (**b**, male) and in adulthood (**c**, male), where the major target of TH axons is the vasculature (examples in **b** and **c** shown by arrows). A sagittal section of the bladder at E18 (**d, e**, female) show the projections to the bladder neck (*bn*) from the adjacent pelvic ganglion (*pg*); blue channel shows DAPI staining to demonstrate organ structures more clearly. **f**, cluster of intramural TH neurons within the E18 bladder muscle (male). **g**, E18 female: NPY axons are present in the muscle where their density is increased in the dorsal region. NPY axons increase in density postnatally (**h**, P2 male) and further increased until adulthood (**i**,

female). In **h**, examples of vascular innervation are indicated by arrows. In **i**, the ureter entry site is indicated by *ur*. Calibration: a-c, e, i 100 μm; d 150 μm; f 30 μm; g, h 175 μm.

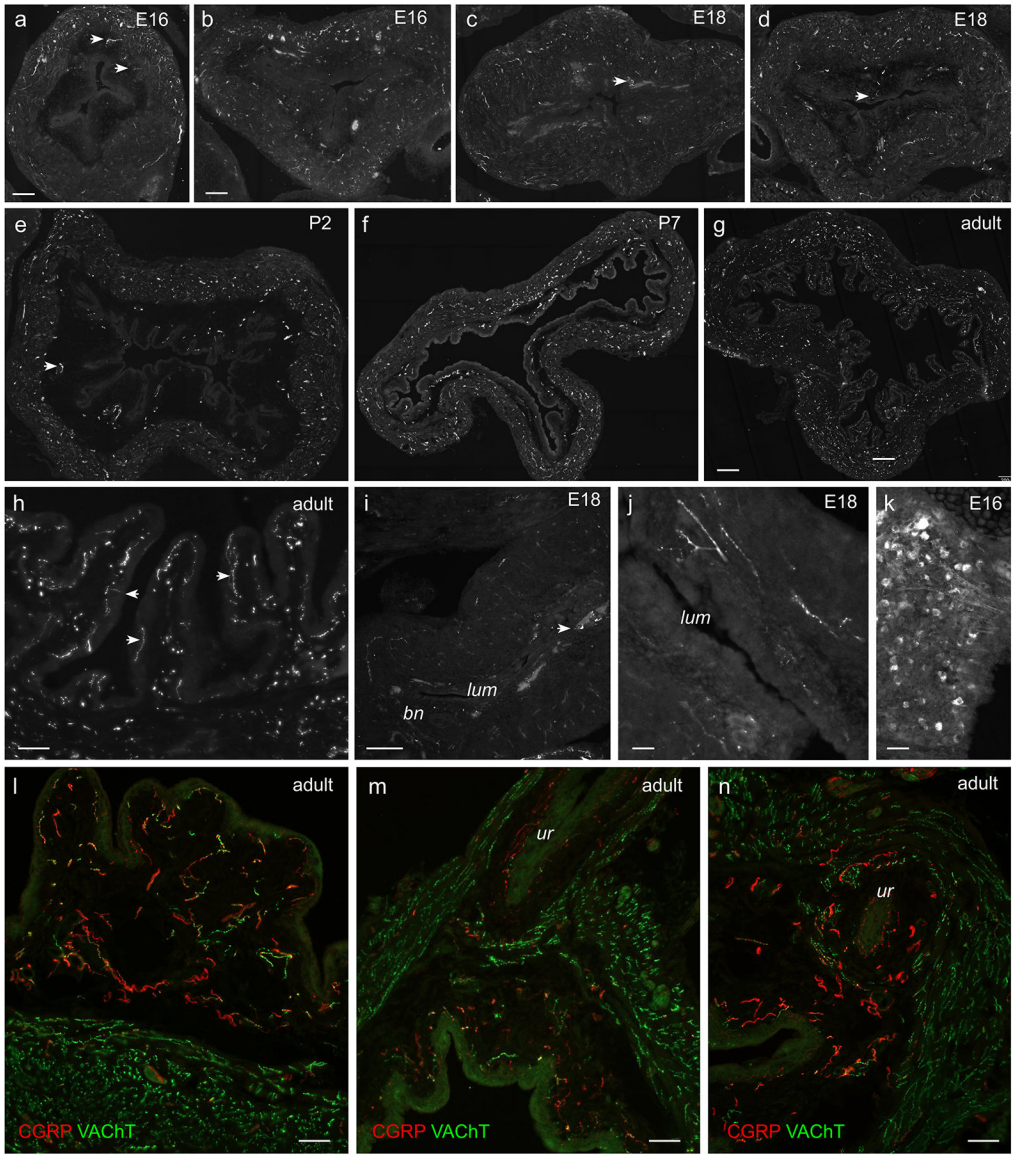

Figure 5: Sensory innervation of the mouse urinary bladder in the pre- and postnatal periods.

Major classes of sensory axons are immunolabelled for CGRP (calcitonin gene-related peptide, **a-h**) and SP (substance P, **i-j**). Panels **a-h** and **l-n** are from bladder sectioned transversely and oriented with dorsal to the top, whereas panels **i** and **j** are from sagittal sections. **a, b**: E16, male, showing sections from the middle of the bladder (**a**) and closer to the bladder neck (**b**), with a progressive increase in CGRP axon density in the muscle towards the bladder neck. Axons in the lamina propria are scarce (examples indicated by arrows). A similar rostrocaudal gradient is evident for CGRP axons at E18 (**c, d**: male); axons in the lamina propria are slightly more common at this time (arrows). Postnatally the innervation of muscle and lamina propria continues to increase (**e**, P2 male; **f**, P7 male; **g**, adult male). **h**, higher magnification of lamina propria in adult male, showing dense innervation by CGRP axons, including axons that lie very close to the urothelium and in some regions penetrate the urothelium (arrows). Sensory axons labelled for SP (**i,**

j) are less prevalent than CGRP axons, shown here at E18 (**i**, female; **j**, male). Arrow in **i** indicates SP axon associated with a blood vessel. Panel **j** shows axons close to the epithelium near the bladder neck. **k**: E16, male; CGRP neuronal cell bodies in a lumbar dorsal root ganglion. **l-n**, adult male bladder, showing distinct tissue innervation by sensory (CGRP) and cholinergic autonomic (VAChT, vesicular acetylcholine transporter axons); **m** and **n** show the ureter entry site at the level of the outer detrusor (**m**) and lamina propria (**n**). Calibration: a, c-e 120 μm; b 100 μm; f 180 μm; g 200 μm; h 40 μm; i, m, n 60 μm; j, k 20 μm; l 80 μm.

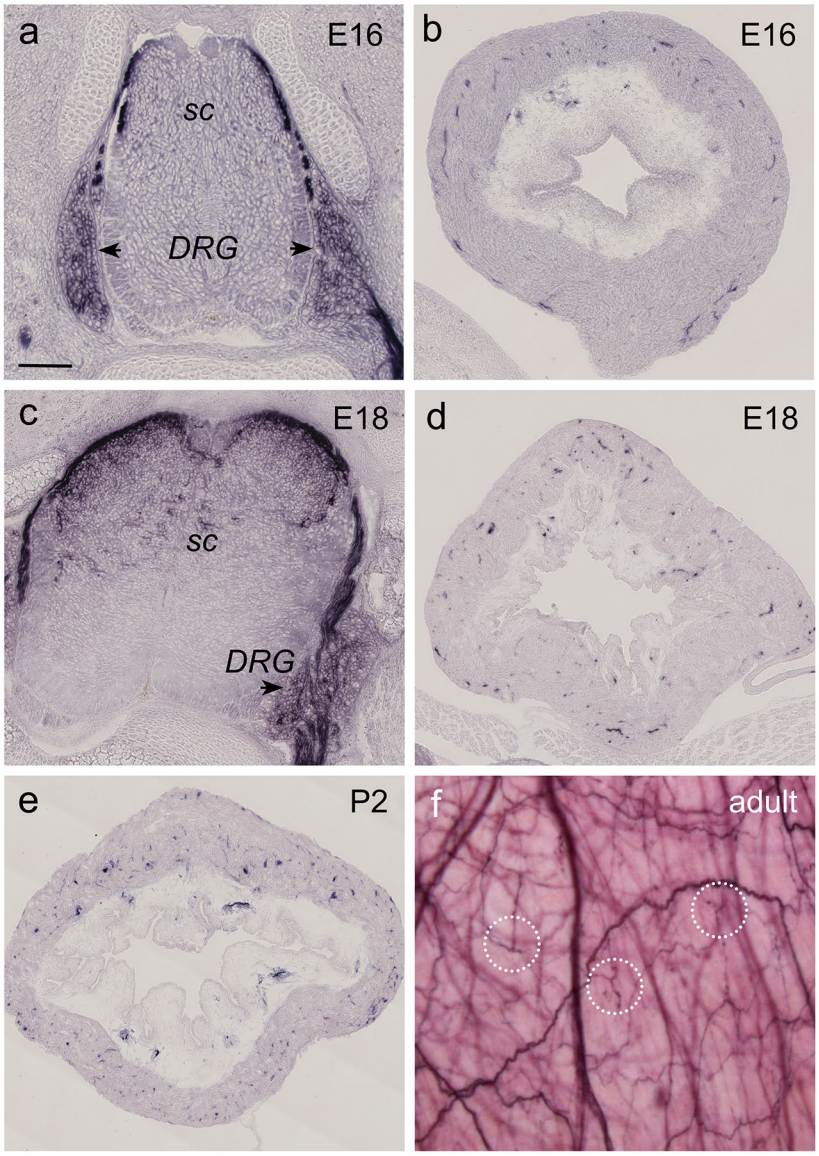

Figure 6: Innervation of the mouse bladder by nociceptive axons in the pre- and postnatal periods.

Histochemical staining for placental alkaline phosphatase visualizes neural structures expressing TRPV1 in tissues dissected from a *Trpv1*$^{PLAP\text{-}nLacZ}$ embryos and postnatal mice. Panels **a-e** are from transverse sections; images oriented with dorsal at the top. **a**, E16 female: TRPV1 sensory labelling of many neurons in dorsal root ganglia (*DRG*; arrows) and projections to the superficial laminae of the spinal cord (*sc*) dorsal horn. **b**, E16, female: TRPV1 axons in the detrusor and lamina propria, both more densely innervated in the dorsal region of the bladder. **c**, E18 female: TRPV1 labeling in sensory neurons of DRG and spinal cord. **d** (E18) and **e** (P2) female bladders, showing increasing density of innervation of muscle and lamina propria, compared with E16. **f**, adult male, whole thickness bladder, showing dense tracts of TRPV1 axons and terminations of single axons (examples circled). Calibration: a, c 100 μm; b 150 μm, d, e 200 μm, f 30 μm.

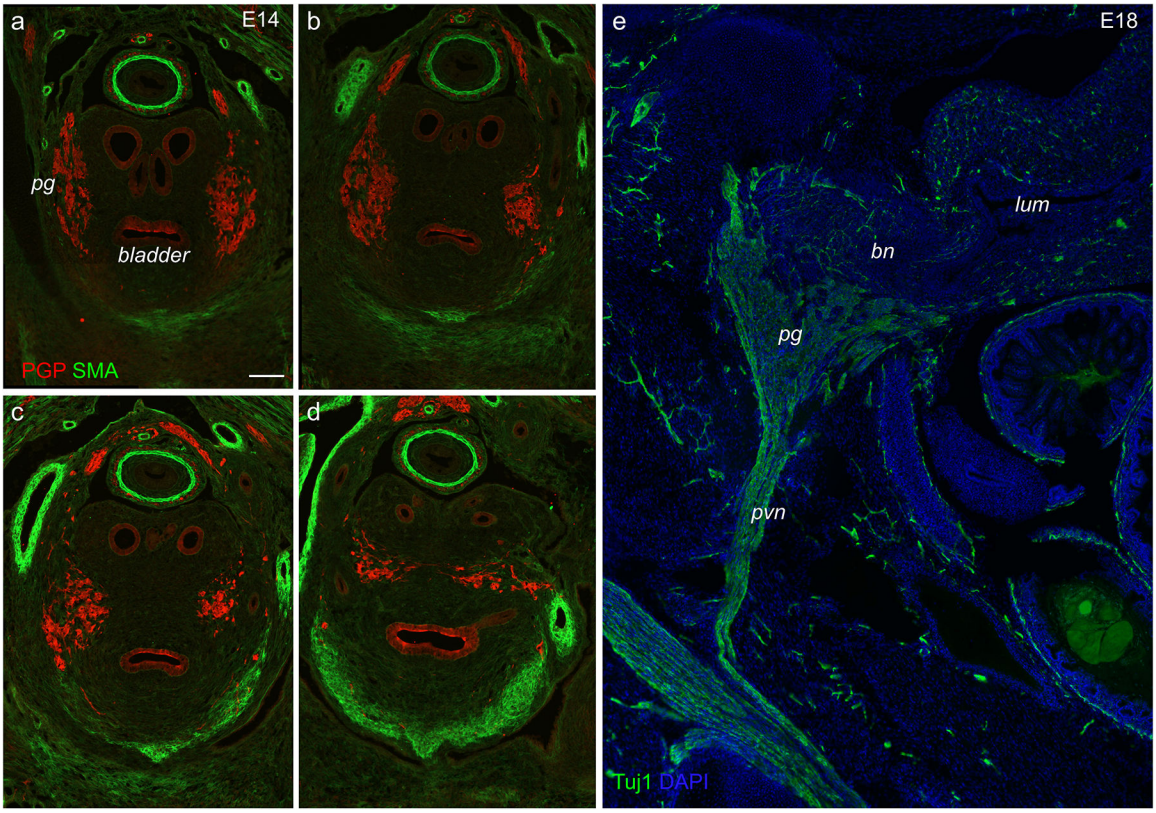

Figure 7: Visualization of pelvic ganglia in embryonic mice.

a-d, E14: transverse sections sampled progressively through the rostrocaudal axis of the bladder show the location of the paired pelvic ganglia (*pg*) and their close apposition to the urogenital tract. Neural tissue is immunolabelled for PGP (protein gene product 9.5, a pan-neural marker); the urothelium of the bladder is also PGP-positive. The developing detrusor muscle on the ventral region of the bladder is identified here with smooth muscle actin (SMA). Sections are ordered from the bladder base to the dome, showing progressive increase in SMA labelling in the bladder. **e**, E18 female: Sagittal section through an embryo at the level of the pelvic ganglion (*pg*), showing its major connection to the sacral cord via the pelvic nerve (*pvn*). This image also shows the extensive neural projections to the bladder; bladder neck (*bn*) and bladder lumen (*lum*) are indicated. Neural tissue is immunolabelled for Tuj1 (class III beta tubulin). In panels a-d, images are oriented with dorsal to the top, whereas panel e is oriented with dorsal to the left. Calibration: a-d 120 μm, e 100 μm.

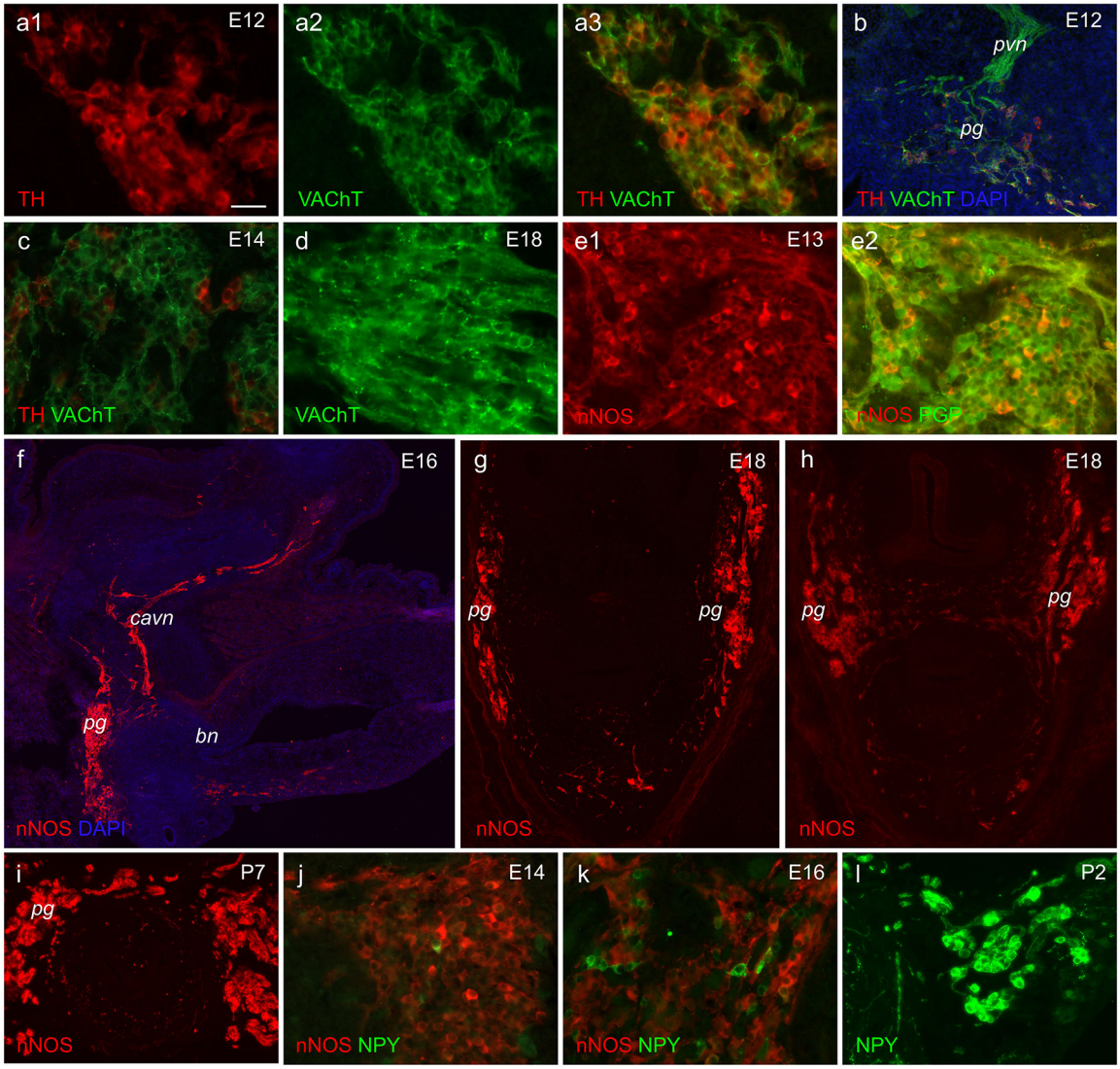

Figure 8: Development and maturation of primary classes of autonomic neurons in mouse pelvic ganglia.

a, E12: Many neurons express TH (tyrosine hydroxylase), a marker of catecholamine synthesis characteristic of noradrenergic neurons; VAChT (vesicular acetylcholine transporter) is also present in many neuronal cell bodies. VAChT-positive axonal boutons are closely associated with many but not all neurons. **b**, E12: sagittal section near the surface of the pelvic ganglion (*pg*), showing the entry of the pelvic nerve (*pvn*). **c**, E14 male: Cholinergic boutons (VAChT) appear similar to the E12 pelvic ganglion, the region shown here containing few noradrenergic (TH) neurons. **d**, E18 female: Compared with E14, cholinergic boutons are more prevalent and clearly distinguished from neuronal somatic labelling. **e**, E13: nNOS (neuronal nitric oxide synthase; nitrergic) is present in a subpopulation of pelvic ganglion neurons and shows diverse intensity of labelling. **f**, E16 male, sagittal section: A large aggregate of nitrergic pelvic ganglion (*pg*) neurons near the bladder neck (*bn*) showing a large projection along the cavernous nerve (*cavn*) to innervate the erectile tissue of the penis. Axon bundles are also evident in the muscle of the bladder,

especially prevalent near the bladder neck. **g-i**, transverse sections showing components of the paired pelvic ganglia that contain numerous nNOS neurons (B, E18 male; **h**, E18 female; **i**, P7 male). **j-l**, neurons labelled for NPY (neuropeptide Y) are scarce at E14 (**j**, female), slightly more common at E16 (**k**, male) and prevalent by P2 (**l**, male). In panel f, image is oriented with dorsal to the left, whereas panels g-i and l are oriented with dorsal to the top. Calibration: a, c, d 20 μm; b, g-i 100 μm, e, j, k 30 μm; f 200 μm, l 50 μm.

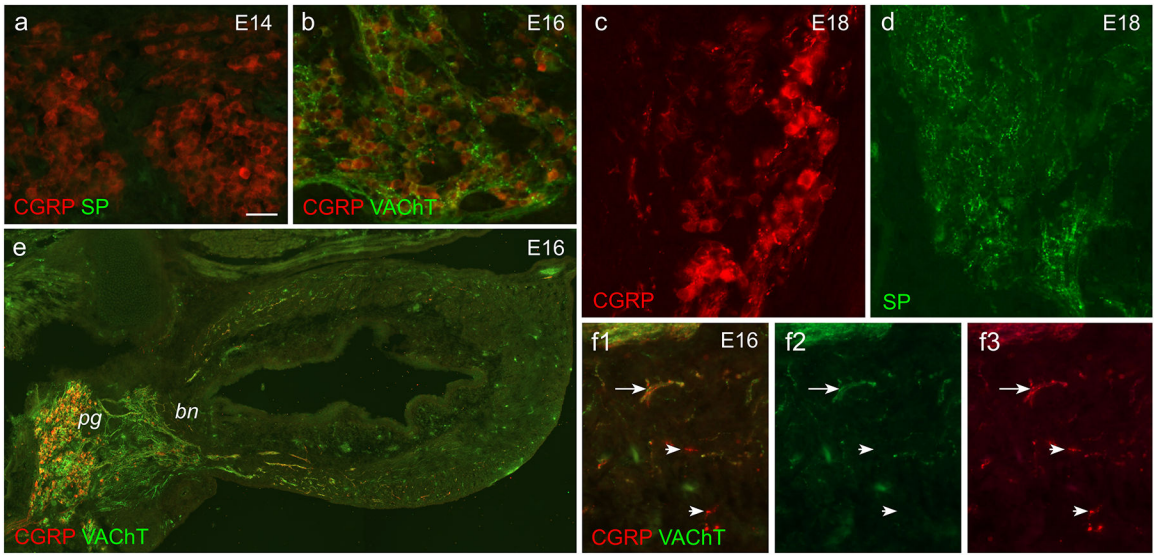

Figure 9: Transient expression of CGRP (calcitonin gene-related peptide) in pelvic ganglia of embryonic mice.

a, E14 female: numerous neuronal cell bodies are show weak to moderate labelling for CGRP, with a several brightly labelled; at this stage no cell bodies or axons are immunoreactive for SP (substance P). **b**, E16 female: CGRP-positive neuronal cell bodies are prevalent and show a range of labelling intensity; many are closely associated with cholinergic (VAChT; vesicular acetylcholine transporter) boutons. **c**, E18 male: intensely labelled CGRP-positive neuronal cell bodies are present but form a minority of the ganglion; by this stage of development, varicose CGRP axons are present in the ganglion and associated with CGRP-positive and -negative cell bodies. **d**, E18 female: numerous SP boutons are present within the ganglion and closely associated with SP-negative cell bodies. **e**, E16 male: sagittal section through the bladder, showing the pelvic ganglia (*pg*) and projections towards the bladder neck (*bn*); the region of pelvic ganglion most distant from the bladder has the highest density of CGRP neurons. **f**, E16 female: Although many pelvic neurons are CGRP-positive at this time, axons double-labelled for VAChT and CGRP are scarce in the bladder. Short arrows show examples of CGRP-positive, VAChT-negative axons and long arrow shows a small bundle of axons that contains separate CGRP and VAChT axons. A very large bundle of axons at the top of the field also contains both axon classes. Calibration: a-d, f 30 μm; e 100 μm.

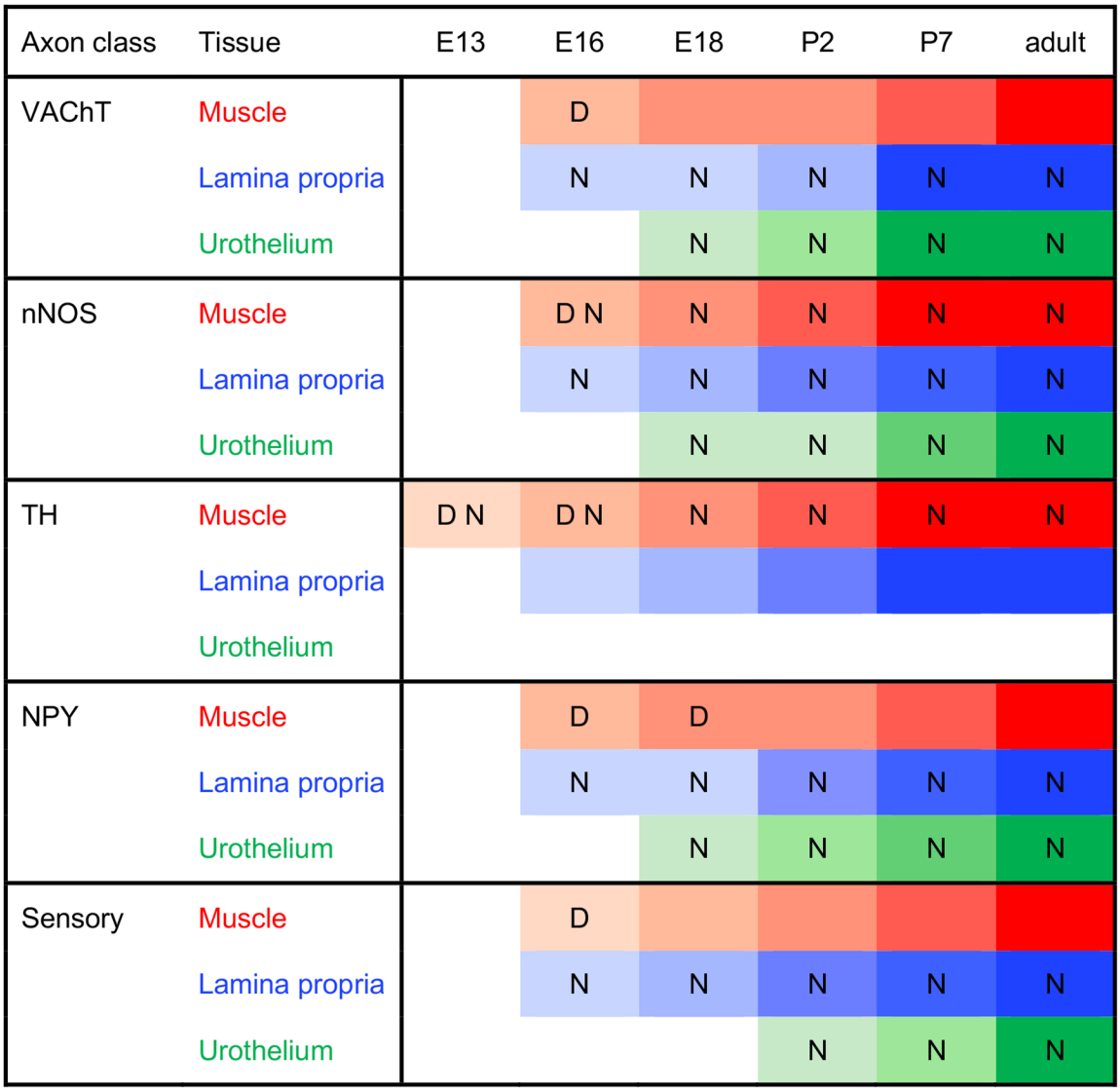

Figure 10: Regional and tissue changes of bladder innervation during mouse development.

For each axon class, the innervation density within a specific tissue is indicated by darkness of the color in that row, from **white** (no innervation) to **darkest** (maximum innervation for that axon class and tissue). In some tissues and at some time points, innervation shows a dorsoventral gradient (indicated **D**), with dorsal regions initially more heavily innervated, or a gradient of increasing innervation density towards the bladder neck (indicated **N**). VAChT (vesicular acetylcholine transporter, cholinergic); nNOS (neuronal nitric oxide synthase, nitrergic); TH (tyrosine hydroxylase, noradrenergic); NPY (neuropeptide Y); Spatiotemporal patterning is similar for CGRP (calcitonin gene-related peptide), SP (substance P) and TRPV1 (nociceptor) populations so aggregated here as ‘sensory’.

Table 1:

Primary antibodies

Antigen	Abbreviation	Host	Company	Item #	RRID	Dilution
Beta tubulin, class III	Tuj1	Rabbit	Biolegend (Covance), San Diego, CA USA	MRB-435P	AB_2564645	1:5000
Calcitonin gene-related peptide	CGRP	Goat	BioRad (AbD Serotec), Gladesville NSW Australia	1720–9007	AB_2290729	1:2000
Calcitonin gene-related peptide	CGRP	Rabbit	Merck (Sigma-Aldrich), North Ryde NSW Australia	C8198	AB_259091	1:5000
Calcitonin gene-related peptide	CGRP	Rabbit	Millipore (Chemicon), Bayswater Vic Australia	AB5920	AB_2068655	1:1000
Nitric oxide synthase 1, neuronal	nNOS	Rabbit	Thermo Fisher (Invitrogen), Scoresby Vic Australia)	61–7000	AB_2533937	1:500
Nitric oxide synthase 1, neuronal	nNOS	Sheep	Gift from Dr P. Emson	H212	AB_2314957	1:5000
Neuropeptide Y	NPY	Rabbit	Immunostar	22940	AB_572253	1:3000
Protein gene product 9.5	PGP9.5	Rabbit	Cederlane Laboratories, Burlington Canada.	CL95101	AB_10548073	1:2000
Smooth muscle actin	SMA	Mouse	Sigma-Aldrich	A5228	AB_630940	1:500
Substance P	SP	Rabbit	Immunostar	20064	AB_572266	1:2000
Tyrosine hydroxylase	TH	Rabbit	Millipore (Chemicon)	AB152	AB_390204	1:2000
Tyrosine hydroxylase	TH	Sheep	Millipore (Chemicon)	AB1542	AB_90755	1:1000
Vesicular acetylcholine transporter	VAChT	Rabbit	Synaptic Systems, Goettingen, Germany	139103	AB_2247684	1:1000